Gyrokinetic large eddy simulations

P. Morel,[1] A. Bañón Navarro,[1] M. Albrecht-Marc,[1] D. Carati,[1] F. Merz,[2]
T. Görler,[2] and F. Jenko,[2]
[1]*Statistical and Plasma Physics Laboratory, Université Libre de Bruxelles, Bruxelles 1050, Belgium*
[2]*Max-Planck-Institut für Plasmaphysik, Boltzmannstr. 2, D-85748 Garching, Germany*

(Received 19 March 2011; accepted 27 May 2011; published online 5 July 2011)

The large eddy simulation approach is adapted to the study of plasma microturbulence in a fully three-dimensional gyrokinetic system. Ion temperature gradient driven turbulence is studied with the GENE code for both a standard resolution and a reduced resolution with a model for the sub-grid scale turbulence. A simple dissipative model for representing the effect of the sub-grid scales on the resolved scales is proposed and tested. Once calibrated, the model appears to be able to reproduce most of the features of the free energy spectra for various values of the ion temperature gradient. © *2011 American Institute of Physics*. [doi:10.1063/1.3601053]

I. INTRODUCTION

Turbulence in plasmas shares several general features with fluid turbulence as modeled by the Navier-Stokes equation. In particular, microturbulence in a background magnetic field as described by the gyrokinetic formalism is thought to be characterized by a forward perpendicular cascade of free energy similar to the direct cascade of kinetic energy in the Richardson-Kolmogorov picture of fluid turbulence.[1–4] Although in plasma microturbulence, there is no inertial range in the strict sense of the word, recent gyrokinetic simulations show that an asymptotically free, self-similar, and highly local cascade develops at high perpendicular wavenumbers.[5] While dissipative processes (due to a coupling to damped eigenmodes[6]) are also active at low wavenumbers, a significant fraction of the free energy is transported to small spatial scales and dissipated there. In a simulation of the complete turbulent cascade process, it is thus important, in principle, to capture all scales from the energy injection range down to the smallest relevant dissipative scales. In certain situations, such direct numerical simulations (DNS) can be computationally expensive or even unfeasible. These DNS limitations have prompted the development of hybrid approaches mixing *ab initio* computation and modeling. In particular, large eddy simulation (LES) techniques have been devised for simulating turbulent fluids at high Reynolds number.[7,8] In these simulations, the large scales are computed explicitly while the influence of the smallest scales is modeled. The aim of the present work is to extend this technique to the gyrokinetic equations which describe the microturbulence in magnetically confined plasmas.[9,10]

As far as fluids are concerned, the main idea behind the development of LES techniques is the assumed existence of a universal regime for the small scales. Indeed, the large scales in a turbulent fluid are very much influenced by the geometry of the flow. It is thus *a priori* not easy, and probably impossible, to design a general model for these large scales. On the contrary, if the Reynolds number is large enough, the smallest scales are supposed to be independent of the geometry and should only be affected by the physical properties of the fluid. Hence, there is a reasonable hope that the small scales can be represented by a general model. In practice, however, the Reynolds number is not always sufficiently large to reach such a regime, and the geometry of wall-bounded flows has to be taken into account in most LES studies of turbulent fluids. Nevertheless, for almost half a century, the LES has proven their ability to significantly decrease the numerical effort required to reproduce the main features of large scale turbulent flows.[7,8] More recently, such methods have also been applied successfully to turbulence in conducting fluids.[11,12]

In the area of gyrokinetic turbulence, the LES techniques have been explored, for instance, by Smith and Hammett,[13] considering hyperviscosity models for two-dimensional drift-wave turbulence—and the aim of the present study is to extend the LES methodology to gyrokinetics in three spatial dimensions. In this context, it should be noted that the plasma microturbulence is different from ordinary fluid turbulence in that it may be driven by various mechanisms such as, e.g., the presence of an ion temperature gradient (ITG) or an electron temperature gradient (ETG). It is expected that the modeling has to be adapted to the drive mechanism (rather than to the geometry of the system). In the present work, we will focus on the case of ITG turbulence.

The paper is organized as follows. The fundamental equations are discussed in Sec. II, and the LES approach for gyrokinetics is presented in Sec. III together with a simple dissipation model. The calibration of the model is discussed for cyclone base case (CBC) parameters which is a standard ITG turbulence test case. An estimate of the truncated scales is proposed for various quantities in Sec. IV. The robustness of the model in terms of parameter changes is analyzed in Sec. V, followed by a summarizing discussion in Sec. VI.

II. GYROKINETIC MODEL

The LES approach can, of course, be studied in the context of a general gyrokinetic system, including multiple

particle species, electromagnetic fluctuations, collisions, general tokamak geometry, profile variations, and the like, as it is generally used in GENE.[14–16] However, in order to simplify the following discussions, we restrict to a reduced system here, working with only one ion species and treating the electrons as adiabatic. At the same time, a simple $\hat{s}$-α model geometry is employed, and collisional effects are neglected. Moreover, the radially local version of GENE is used which solves the gyrokinetic equations in a flux-tube geometry,[17,18] employing the field-aligned coordinates $(x, y, z, v_\parallel, \mu)$. The derivation of the corresponding non-dimensional equations can be found in previous studies.[16] The resulting expressions read as follows. The time evolution of the ion distribution function f_{ki} in k space is given by

$$\partial_t f_{ki} = L[f_{ki}] + N[f_{ki}, f_{ki}] + D[f_{ki}], \tag{1}$$

where the linear term can be split into three contributions, $L[f_{ki}] = L_G[f_{ki}] + L_C[f_{ki}] + L_\parallel[f_{ki}]$, with

$$L_G[f_{ki}] = -\left(\omega_{ni} + \left(v_\parallel^2 + \mu B_0 - 3/2\right)\omega_{Ti}\right) F_0 i k_y (J_0 \phi_k),$$

$$L_C[f_{ki}] = -\frac{T_{0i}(2v_\parallel^2 + \mu B_0)}{Z_i T_{0e} B_0}(K_x i k_x h_{ki} + K_y i k_y h_{ki}),$$

$$L_\parallel[f_{ki}] = -\frac{v_{Ti}}{2}\left(\partial_z \ln F_0\, \partial_{v_\parallel} h_{ki} - \partial_{v_\parallel} \ln F_0\, \partial_z h_{ki}\right).$$

Here, h_{ki} is defined as the nonadiabatic part of the distribution function, $h_{ki} = f_{ki} + Z_i F_{0i} \phi_k T_{0e}/T_{0i}$, where Z_i denotes the charge number, F_{0i} the background distribution function, ϕ the electrostatic potential, B_0 the magnetic field, and T_{0e}, T_{0i} the electron and ion temperatures. The first linear term L_G represents the influence of the fixed logarithmic ion density (ω_{ni}) and temperature (ω_{Ti}) gradients expressed in major radius R_0 units, the second linear term L_C describes the effects due to magnetic curvature (with K_x and K_y the standard curvature terms[18]), and the third linear term $L_\parallel$ contains the parallel dynamics involving magnetic trapping as well as the linear Landau damping. The nonlinear term N represents the effect of the self-consistent electric field in the $\vec{E} \times \vec{B}$ drift of charged particles,

$$N[f_{ki}, f_{ki}] = \sum_{k'} \left(k'_x k_y - k_x k'_y\right) J_0 \phi_{k'} f_{(k-k')i},$$

and the dissipation term $D[f_{ki}]$ is given by

$$D[f_{ki}] = -\left(a_x (i\,k_x)^n + a_y (i\,k_y)^n + a_z\, \partial_z^n + a_{v_\parallel}\, \partial_{v_\parallel}^n\right) f_{ki},$$

where typically $n = 4$ is used, and the coefficients a_x, a_y, a_z, and $a_{v_\parallel}$ can be adapted to each specific class of physical problems. In the local version of GENE used here, unknown genes are Fourier transformed in the radial and poloidal directions so that x and y are replaced, respectively, by k_x and k_y. The subscript 'k' has been added to label such Fourier space quantities. Due to the imposed quasi-neutrality, the electrostatic potential ϕ and the distribution function are related via the linear equation

$$\begin{aligned} Z_i^2 n_{0i} \frac{T_{0e}}{T_{0i}}(1 - \Gamma_0(b_i))\phi_k + n_{0e}(\phi_k - \langle \phi_k \rangle_{FS}) \\ = Z_i n_{0i} \pi B_0 \int d\mu\, dv_\parallel\, J_0(\lambda) f_{ki}\,, \end{aligned} \tag{2}$$

with $\lambda^2 = 2k_\perp^2 \mu/B_0$ and $b_i = v_{Ti}^2 k_\perp^2/(2\Omega_{ci}^2)$. The functions J_0 and $\Gamma_0(b_i) = \exp(-b_i)\, I_0(b_i)$ are, respectively, the Bessel and the scaled modified Bessel functions of order zero, where Ω_{ci} is the ion cyclotron pulsation, v_{Ti} is their thermal velocity, ρ_i is their Larmor radius, and $q_i = Z_i e$ is their charge. The electron and ion equilibrium densities are, respectively, n_{0e} and n_{0i}. In the flux-tube geometry (symbolically defined by the metric coefficients[18] g^{xx}, g^{xy}, and g^{yy} and by the smallness parameters $\epsilon_{R_0} = \rho_i/R_0$), the amplitude of the perpendicular wave vector $k_\perp$ is given by $k_\perp^2 = g^{xx}k_x^2 + 2g^{xy}k_x k_y + g^{yy}k_y^2$ and depends on z through the metric coefficients. Note that $\langle \phi \rangle_{FS}$ represents the flux surface average of the electric potential.

One property of the gyrokinetic equations which is of particular interest here is the conservation of the free energy by the nonlinear term.[1,19,20] The latter quantity is defined as

$$\mathcal{E} = n_{0i} \frac{T_{0i}}{T_{0e}} \int d\Lambda_k \frac{h_{-ki} f_{ki}}{2F_{0i}}, \tag{3}$$

where $h_{-ki} = h_i(-k_x, -k_y, z, v_\parallel, t)$. The integration over the phase space of a given quadratic unknown $|X_k|^2 = X(k_x, k_y, z, v_\parallel, \mu, t) X(-k_x, -k_y, z, v_\parallel, \mu, t)$ is given by

$$\int d\Lambda_k\, |X_k|^2 = \frac{1}{V} \sum_{k_x^{\mathrm{DNS}}} \sum_{k_y^{\mathrm{DNS}}} \int \pi\, dz\, dv_\parallel\, d\mu\, |X_k|^2, \tag{4}$$

where the sum over k_x^{DNS} has to be understood as a sum from $k_x = (-N_x/2 + 1)\Delta k_x$ to $k_x = N_x/2\Delta k_x$ and the sum over k_y^{DNS} corresponds to a sum from $k_y = (-N_y/2 + 1)\Delta k_y$ to $k_y = N_y/2\Delta k_y$. Here, $\Delta k_x = 2\pi/L_x$ and $\Delta k_y = 2\pi/L_y$ are the smallest wave vectors that can be used to represent periodic functions in rectangular domain of size $L_x \times L_y$. In practice, due to the symmetry of Fourier transform, negative k_y modes are given by complex conjugation of positive k_y modes. The volume V is defined in the chosen magnetic $\hat{s} - \alpha$ equilibrium by

$$V = \sum_{k_x^{\mathrm{DNS}}} \sum_{k_y^{\mathrm{DNS}}} \int dz/B_0. \tag{5}$$

The two-dimensional spectral density of the free energy is defined by

$$\mathcal{E}^{k_x,k_y} = \frac{n_{0i}\, T_{0i}}{V\, T_{0e}} \int \pi dz dv_\parallel d\mu \left(\frac{h_{-ki} f_{ki}}{2F_{0i}}\right), \tag{6}$$

and the one-dimension spectral densities along k_x or k_y are simply given by

$$\mathcal{E}^{k_x} = \sum_{k_y^{\mathrm{DNS}}} \mathcal{E}^{k_x,k_y}, \quad \mathcal{E}^{k_y} = \sum_{k_x^{\mathrm{DNS}}} \mathcal{E}^{k_x,k_y}.$$

The free energy balance can be expressed as follows:

$$\partial_t \mathcal{E} = \mathcal{G} - \mathcal{D}. \tag{7}$$

The two terms in the right hand side represent the free energy injection $\mathcal{G}$ and dissipation $\mathcal{D}$. They are given by

$$\mathcal{G} = n_{0i}\frac{T_{0i}}{T_{0e}}\int d\Lambda_k \frac{h_{-ki}}{F_{0i}} L_G[f_{ki}], \tag{8}$$

$$\mathcal{D} = -n_{0i}\frac{T_{0i}}{T_{0e}}\int d\Lambda_k \frac{h_{-ki}}{F_{0i}} D[f_{ki}]. \tag{9}$$

The free energy injection term $\mathcal{G}$ is directly related to the ion heat flux, $\mathcal{Q}_i$,

$$\mathcal{G} = \omega_{Ti}\mathcal{Q}_i. \tag{10}$$

The heat diffusivity χ_i and heat flux $\mathcal{Q}_i = n_{0i}T_{0i}\omega_{Ti}\chi_i$ are considered as reference quantities for comparison between gyrokinetic numerical solvers as well as with experiments. The appearance of heat flux as the free energy source stresses the importance of free energy balance in gyrokinetics.

III. LES FOR GYROKINETICS

The main objective of the LES technique is to explore the large scale physics at a lower computational cost when compared to the DNS. Reducing the cost of a gyrokinetic simulation can be achieved by several ways. In an Eulerian approach, the distribution function is represented on a fixed grid in five-dimensional phase space, using $N_x \times N_y \times N_z \times N_{v_\parallel} \times N_\mu$ grid points. In a gyrokinetic LES, this grid is then to be coarsened. Considering that the perpendicular cascade processes have been shown[5] to transfer the free energy from large spatial scales to small ones, this technique is limited here to a filtering of the (x,y) grid. In the following, the DNS and LES grids correspond, respectively, to $N_x \times N_y = 128 \times 64$ and $\bar{N}_x \times \bar{N}_y = 48 \times 24$, while $N_z = 16$, $N_{v_\parallel} = 32$, and $N_\mu = 8$ are held constant. The coarsening of the grid can be viewed as a low pass filter, denoted hereafter by the $\bar{\cdot}$ symbol, that sets to zero, the highest k_x and k_y modes. In the test-case treated in this paper, the spatial directions perpendicular to the magnetic field are clearly the most demanding in terms of grid points. This situation thus motivates the choice to focus the filtering effort on these two directions. However, it has also been shown in two-dimensional slab ITG turbulence,[21] that the distribution along $v_\parallel$ can be expanded as a series of Hermitian polynomial and that a cascade process is observed towards the higher order polynomials. Such a velocity space cascade could also be considered to reduce the resolution in $v_\parallel$. This choice has, however, not been retained here, mainly for two practical reasons. First, the resolution in $v_\parallel$ is not very high, and second, the discretisation along $v_\parallel$ is based on finite differences instead of a Hermite polynomials expansion. The filtered distribution function will thus be labeled $\bar{f}_{ki}$. Applying this filter to the gyrokinetic equation yields

$$\partial_t \bar{f}_{ki} = L[\bar{f}_{ki}] + N[\bar{f}_{ki},\bar{f}_{ki}] + D[\bar{f}_{ki}] + \bar{T}, \tag{11}$$

which contains a term $\bar{T}$ that depends explicitly on both the filtered distribution $\bar{f}_{ki}$ and on the unfiltered distribution f_{ki}

$$\bar{T} = \overline{N[f_{ki},f_{ki}]} - N[\bar{f}_{ki},\bar{f}_{ki}]. \tag{12}$$

Except for the presence of $\bar{T}$ on the right hand side, Eq. (11) for $\bar{f}_{ki}$ has the same form as Eq. (1) for f_{ki}. The term $\bar{T}$ is usually referred to as the sub-grid scale term, though in the present situation, the terminology sub-filter scale term would be more appropriate. In order to close Eq. (11), $\bar{T}$ must be approximated by a model that has to be expressed in terms of the filtered distribution $\bar{f}_{ki}$,

$$\bar{T} \approx M[\bar{f}_{ki}]. \tag{13}$$

The importance of the sub-grid scale term is illustrated in Fig. 1. Two free energy spectra are represented for the CBC (Ref. 22) for ITG driven turbulence ($\omega_{ni} = 2.22$, $\omega_{Ti} = 6.92$, $q = 1.4$, $\hat{s} = 0.796$, $\epsilon = 0.18$, $T_{e0}/T_{i0} = 1$, and $Z_i = 1$). The perpendicular box sizes are given by $L_x = L_y = 125\rho_i$. In GENE, numerical dissipation[23] can be introduced via fourth-order derivatives along z and $v_\parallel$,

$$D[f_{ki}] = -a_z\partial_z^4 f_{ki} - a_{v_\parallel}\partial_{v_\parallel}^4 f_{ki}, \tag{14}$$

where the values for the coefficients a_z and $a_{v_\parallel}$ are to be adjusted appropriately. In the following, $a_z = a_{v_\parallel} = 1.0$ while $a_x = a_y = 0.0$. It should be emphasized that these values have been obtained using a trial and error process. The optimal values for $a_z = a_{v_\parallel} = 1.0$ have been found to be robust for the parameter regime studied here.[23] On the contrary, the perpendicular coefficients a_x, a_y depend strongly on the physics involved. In a certain sense, the dissipation term can be viewed as a sub-grid scale model. In the following, the model that is proposed is actually very much inspired by the structure of D.

In Fig. 1, the DNS spectrum is compared to the LES spectrum obtained by setting $\bar{T} = 0$. Clearly, the free energy is piling up in the high k_x range in the latter case due to the reduced high-wavenumber dissipation in the absence of small scales. As a secondary effect, the free energy appears

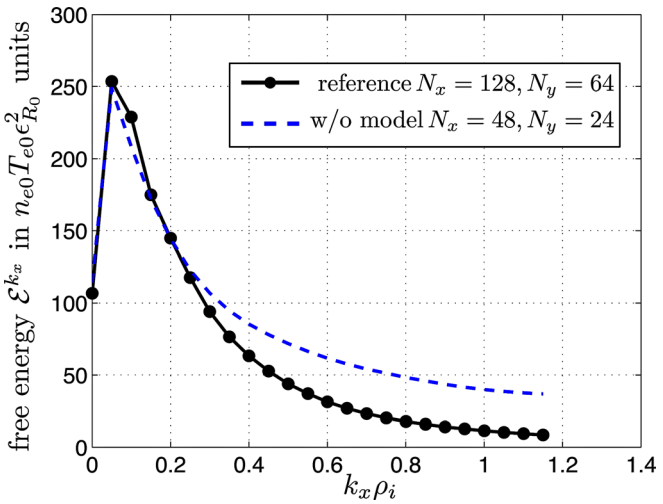

FIG. 1. (Color online) Free energy: Comparison between highly resolved DNS (black •) and LES without model (blue ---) for the cyclone base test case. The resolution for the DNS is $N_x = 128$ and $N_y = 64$ and for the LES is $N_x = 48$ and $N_y = 24$.

to be pumped out more rapidly of the large scales where the gradient source term is active. Indeed, the free energy is transferred to the small scales by the nonlinear term. These transfers have been identified as mostly local in Fourier space.[5] Consequently, the increase of activity of modes closer to the injection range can explain that the free energy is removed from the drive range more rapidly. Such a scenario is reminiscent of what is observed in under-resolved DNS of Navier-Stokes turbulence, where the energy is also piling up in the large wavenumber range.

In Fig. 1, the LES has been performed with $\bar{T}=0$, which can be considered as the simplest sub-grid scale model. Obviously, such a choice is too simple since the free energy spectrum deviates significantly from the DNS observations. The role of $\bar{T}$ can be understood by considering the resolved free energy balance. Since f_{ki} and $\bar{f}_{ki}$ satisfy the same equation up to the term $\bar{T}$, the free energy associated to $\bar{f}_{ki}$, referred to as the resolved free energy in the framework of a LES, must satisfy the following equation

$$\partial_t \overline{\mathcal{E}} = \overline{\mathcal{G}} - \overline{\mathcal{D}} - \overline{\mathcal{T}}, \tag{15}$$

where the quantities $\overline{\mathcal{E}}$, $\overline{\mathcal{G}}$, $\overline{\mathcal{D}}$ are the same as $\mathcal{E}$, $\mathcal{G}$, $\mathcal{D}$, except that they are defined using $\bar{f}_{ki}$ and $\bar{h}_{ki}$ instead of f_{ki} and h_{ki}. It should be noted, however, that all these global quantities are defined using a volume integration over $d\bar{\Lambda}_k$ in which the sums are over k_x^{LES} and k_y^{LES} and have to be understood as a sum from $k_x=(-\bar{N}_x/2+1)\,\Delta k_x$ to $k_x=\bar{N}_x/2\,\Delta k_x$ and from $k_y=(-\bar{N}_y/2)\,\Delta k_y$ to $k_y=\bar{N}_y/2\,\Delta k_y$. Since the computational box sizes are the same in the LES and in the reference DNS, the same grid spacings Δk_x and Δk_y are used in both LES and DNS runs. However, the largest wave vectors are smaller in the LES than in the DNS: $K_x^{\mathrm{LES}}=\bar{N}_x/2\Delta k_x < K_x^{\mathrm{DNS}}=N_x/2\Delta k_x$ and $K_y^{\mathrm{LES}}=\bar{N}_y/2\Delta k_y < K_y^{\mathrm{DNS}}=N_y/2\Delta k_y$. The new term $\mathcal{T}_{\bar{T}}$ is defined by

$$\mathcal{T}_{\bar{T}} = -\int d\bar{\Lambda}_k\, n_{0i}\frac{T_{0i}}{T_{0e}}\frac{\bar{h}_{-ki}}{F_{0i}}\,\bar{T} \tag{16}$$

and represents the effect of the sub-grid scales on the resolved free energy. If the cascade picture applies, the effect of the $\mathcal{T}_{\bar{T}}$ should be to pump out the resolved free energy in order to mimic the transfer towards the unresolved scales. If f_{ki} and h_{ki} are known from a DNS, the term $\bar{T}$ and consequently $\mathcal{T}_{\bar{T}}$ can be computed exactly. Using the same parameter as in Fig. 1, $\mathcal{T}_{\bar{T}}$ has been computed and is shown in Fig. 2. It is indeed negative and represents a loss of resolved free energy. Its amplitude is compared to the resolved free energy injection rate $\mathcal{G}_{\bar{f}}$ and dissipation rate $\mathcal{D}_{\bar{f}}$. On average, once turbulence is developed and a statistically stationary regime is reached, these three terms should be in balance, $\mathcal{G}_{\bar{f}}\approx\mathcal{D}_{\bar{f}}+\mathcal{T}_{\bar{T}}$. In the run corresponding to Fig. 1, the ratio $\mathcal{T}_{\bar{T}}/\mathcal{D}_{\bar{f}}$ appears to be close to unity. Hence, the transfer of free energy between the resolved and the unresolved scales cannot be neglected.

The development of models for representing the effect of small, under-resolved scales on the large, resolved scales has been the subject of countless efforts in LES for fluid turbulence. However, the most commonly used models simply

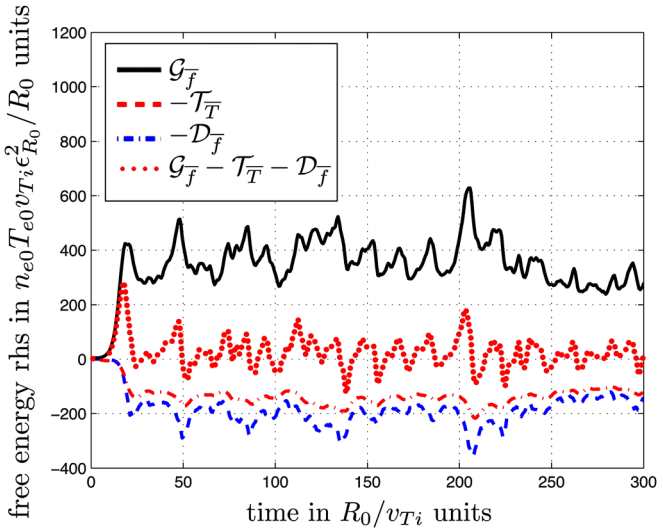

FIG. 2. (Color online) Sub grid contribution to the free energy balance compared with the free energy injection and dissipation terms. CBC parameters with a filter corresponding to $\bar{N}_x=48$, $\bar{N}_y=24$.

attempt to reproduce the transfer of kinetic energy towards the unresolved scales by a dissipative mechanism usually represented by an effective viscosity. Considering the analogy between fluid and plasma turbulence, it is proposed here to also use an effective dissipation which is modeled by the hyper-diffusion term

$$M[\bar{f}_{ki}] = -c_\perp k_\perp^4 \bar{h}_{ki}. \tag{17}$$

It is easy to verify that such a model always gives a negative contribution to the resolved free energy balance,

$$\begin{aligned}\mathcal{T}_M &= -n_{0i}\frac{T_{i0}}{T_{e0}}\int d\bar{\Lambda}_k \frac{\bar{h}_{-ki}}{F_{0i}} M[\bar{h}_{ki}] \\ &= -c_\perp n_{0i}\frac{T_{i0}}{T_{e0}}\int d\bar{\Lambda}_k \left|\frac{k_\perp^2\bar{h}_{ki}}{\sqrt{F_{0i}}}\right|^2 < 0.\end{aligned} \tag{18}$$

The hyper-diffusion coefficient $c_\perp$ can be adjusted by comparing the results given by a reference (well resolved) DNS with results from a LES using Eq. (18). The $k_\perp^4$ dependency in Eq. (17) might be surprising since the micro-turbulence is known to be anisotropic, as it is illustrated by the existence of large scale structures like zonal flows or streamers. However, there is evidence that turbulence appears to be very close to isotropy in the plane perpendicular to the magnetic field at scales smaller than the driving range.[24] Also, the power four dependence is not trivial at all. It must be acknowledged at this point that no strong theoretical support can be given to this choice. At least one other choice ($\propto k_\perp^2$) has been tested but led to slightly less satisfactory results and is not discussed further here.

In Fig. 3, the free energy spectra $\mathcal{E}^{k_x}$ and $\mathcal{E}^{k_y}$ are displayed for various values of $c_\perp$. The black curve corresponds to the reference DNS run. It is compared to four LES runs corresponding to $c_\perp=\{0, 0.025, 0.375, 1.0\}$. Other values of $c_\perp$ have also been tested but are not shown here for clarity. All the spectra are time-averaged during the turbulent phase over a period of $2000R_0/v_{Ti}$. Obviously,

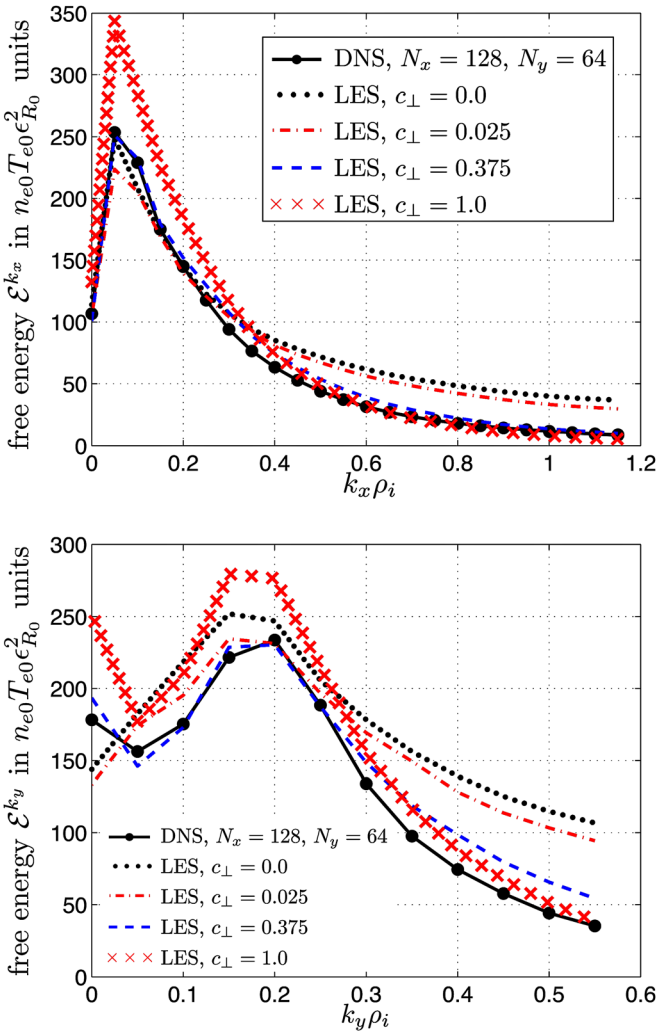

FIG. 3. (Color online) Resolved free energy spectra $\mathcal{E}^{k_x}$ (top) and $\mathcal{E}^{k_y}$ (bottom) obtained by varying the model coefficient compared with reference DNS.

a too small parameter ($c_\perp = 0.025$ dash-dotted) does not significantly improve the result when compared to the no-model case ($c_\perp = 0$ dotted). Also, a too large value of $c_\perp$ ($\times$ dotted) tends to over-damp the small scales which leads to an artificial accumulation of free energy in the large scales (small k). The optimal value appears to be close to $c_\perp = 0.375$ (dashed). The corresponding LES reproduces fairly well the spectra of the resolved free energy both in k_x and in k_y.

The model has been calibrated for a given perpendicular grid $N_x = 48$, $N_y = 24$. Its robustness can then be tested by varying the number of grid points. Such a study is illustrated in Fig. 4. It is noted that the results are not significantly modified for the resolutions considered here, namely, from ($N_x = 64$, $N_y = 32$) down to ($N_x = 40$, $N_y = 20$). The minimal grid resolution ($N_x = 40$, $N_y = 20$) appears to be very close to the grid retained in the systematic study discussed in Sec. IV ($N_x = 48$, $N_y = 24$). Considering the quite low resolutions used here in the DNS and in the LES, it is, however, probably quite dangerous to draw any strong conclusion on the convergence properties of gyrokinetic LES from this single study.

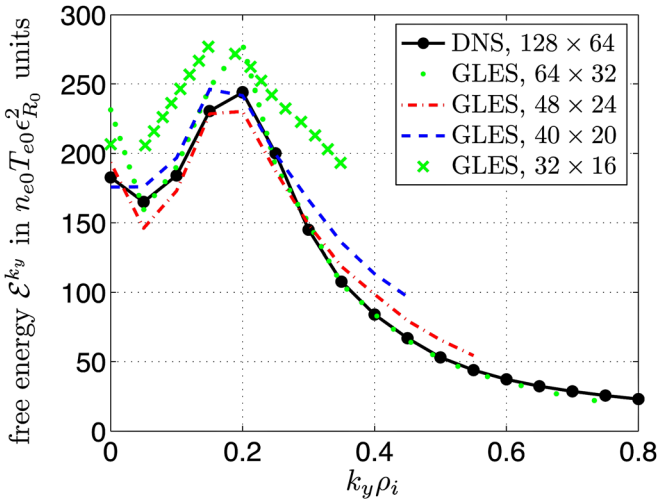

FIG. 4. (Color online) Resolved free energy spectrum $\mathcal{E}^{k_y}$ obtained by varying the number of perpendicular grid points. $\mathcal{E}^{k_x}$ spectrum shows the same features and has been removed for clarity.

IV. ESTIMATE FOR THE SUB-GRID QUANTITIES

The use of a model has been shown in Sec. III to improve significantly the agreement between DNS and LES in gyrokinetic simulations. In terms of free energy, the effect of the model (17) used in the LES is expressed by the formula (18). This quantity can also be computed in a filtered DNS by using the knowledge of all the modes,

$$\mathcal{T}_{\bar{\mathcal{I}}}^{k_x,k_y} = \sum_{k_x',k_y' > K_x^{\mathrm{LES}},K_y^{\mathrm{LES}}} \mathcal{T}_{\bar{\mathcal{I}}}^{k_x,k_y,k_x',k_y'}, \tag{19}$$

where the four-dimensional quantity $\mathcal{T}_{\bar{\mathcal{I}}}^{k_x,k_y,k_x',k_y'}$ arises from the non-linearity and can be interpreted as a nonlinear transfer function from modes (k_x', k_y') to modes (k_x, k_y).[5]

A comparison between $\mathcal{T}_{\bar{\mathcal{I}}}^{k_x,k_y}$ and $\mathcal{T}_{M}^{k_x,k_y}$ is shown in Fig. 5. The model presents an overall surprisingly good agreement with the sub-grids spectra obtained from the DNS, while the detailed structure is smoothed down by the model.

Since small scales are truncated in the LES runs, it is not possible in LES to predict directly global quantities such as the total free energy, the total heat flux (or equivalently, the total free energy injection), and the total free energy dissipation. An estimate of the contribution from the truncated scales to these global quantities is certainly desirable if a comparison has to be made with experimental results.

In this section, a simple estimate is proposed for the sub-grid scale contribution to these quantities. It is noted that all these quantities ($\mathcal{E}$, $\mathcal{G}$, or $\mathcal{D}$), generically represented by Q, can be represented either by their two-dimensional spectrum Q^{k_x,k_y} or by their one-dimensional k_x spectrum $\left(Q^{k_x}\right)$ and k_y spectrum $\left(Q^{k_y}\right)$. In a LES, only the resolved part of Q, denoted hereafter $\bar{Q}$, is directly accessible. It is given by

$$\bar{Q} = \sum_{|k_x| \le K_x^{\mathrm{LES}}} Q^{k_x} = \sum_{|k_y| \le K_y^{\mathrm{LES}}} Q^{k_y}. \tag{20}$$

The unresolved part of Q, denoted δQ, contains three contributions $\delta Q = \delta_x Q + \delta_y Q + \delta_{xy} Q$,

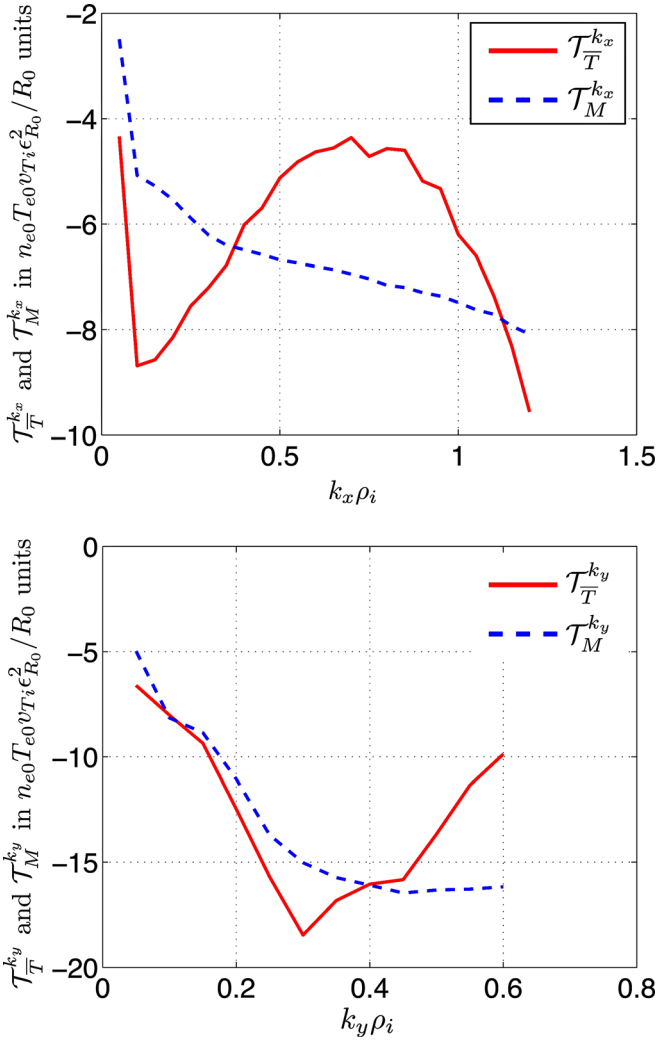

FIG. 5. (Color online) Resolved sub-grids spectra $\mathcal{T}_T^{k_x}$ (top) and $\mathcal{T}_T^{k_y}$ (bottom) compared with dissipations due to model $\mathcal{T}_M^{k_x}$ and $\mathcal{T}_M^{k_y}$.

$$\delta_x Q = \sum_{|k_x|>K_x^{\mathrm{LES}}} \sum_{|k_y|\le K_y^{\mathrm{LES}}} Q^{k_x,k_y}, \tag{21}$$

$$\delta_y Q = \sum_{|k_x|\le K_x^{\mathrm{LES}}} \sum_{|k_y|>K_y^{\mathrm{LES}}} Q^{k_x,k_y}, \tag{22}$$

$$\delta_{xy} Q = \sum_{|k_x|>K_x^{\mathrm{LES}}} \sum_{|k_y|>K_y^{\mathrm{LES}}} Q^{k_x,k_y}. \tag{23}$$

In DNS, δQ can be computed, but in LES, it has to be estimated. Such an estimate can be obtained by noting that, in the large k_x and k_y ranges of LES runs, the quantity Q can often be approximated by decaying power laws,

$$Q^{k_x} \approx A_x\, k_x^{-\alpha_x}, \quad Q^{k_y} \approx A_y\, k_y^{-\alpha_y}. \tag{24}$$

The amplitudes A_x and A_y as well as the exponents α_x and α_y can be estimated by linear regression from the LES spectra. In that case, the following estimates can be obtained,

$$\delta_x Q \approx \sum_{|k_x|>K_x^{\mathrm{LES}}}^{K_x^{\mathrm{DNS}}} A_x\, k_x^{-\alpha_x}, \tag{25}$$

$$\delta_y Q \approx \sum_{|k_y|>K_y^{\mathrm{LES}}}^{K_y^{\mathrm{LES}}} A_y\, k_y^{-\alpha_y}. \tag{26}$$

Since these sums are finite, there is *a priori* no restriction on the values of the exponents. However, if the wave vector range is extended to infinity, these sums converge if and only if $\alpha_x > 1$ and $\alpha_y > 1$. Estimating $\delta_{xy}Q$ is more difficult. However, assuming a separable spectrum $Q^{k_x,k_y} = q_1^{k_x} q_2^{k_y}$, it can be shown that $\delta_{xy}Q = \delta_x Q\, \delta_y Q/\bar{Q}$. In general, it is thus expected that the correction due to $\delta_{xy}Q$ is very small and can be neglected compared to $\delta_x Q$ or $\delta_y Q$. This procedure has been used to estimate the total value of both the free-energy and the heat flux from the LES with the optimal value of $c_\perp$ and from the LES without model.

As far as the free energy is concerned, the best fit of the one-dimensional spectra yields $\alpha_x = 2.21$ and $\alpha_y = 1.74$ for $c_\perp = 0.375$. These values are then used to compute the corrections $\delta_x\mathcal{E}$ and $\delta_y\mathcal{E}$. The LES estimate $\mathcal{E}^{\mathrm{LES}}$ for the total free energy can then be compared to the value measured from the DNS, $\mathcal{E}^{\mathrm{DNS}}$. It is found that the LES estimate is in good agreement with the DNS value $\mathcal{E}^{\mathrm{LES}} = 1.10\mathcal{E}^{\mathrm{DNS}}$. On the contrary, without a model ($c_\perp = 0$), the best fit of the free-energy one dimensional spectra yields $\alpha_x = 0.79$ and $\alpha_y = 0.85$. In that case, the estimates (25) and (26) would be divergent if the sums had to be extended to infinity. However, if the sums are limited to K^{DNS}, it is possible to reconstruct the total free energy from the LES without model, but the estimate is more than twice the value of the DNS: $\mathcal{E}^{\text{No Model}} = 2.1\ \mathcal{E}^{\mathrm{DNS}}$.

The same procedure has been used for the free energy injection $\mathcal{G} = \omega_{Ti}\,\mathcal{Q}_i$ (Fig. 6). For $c_\perp = 0.375$, the regression method yields $\alpha_x = 3.60$ and $\alpha_y = 2.20$, which gives the following estimate $\mathcal{G}^{\mathrm{LES}} = 1.11\ \mathcal{G}^{\mathrm{DNS}}$. Again, the value computed from the LES slightly overestimates the DNS value of the free energy injection. However, this prediction is still in reasonable agreement with the DNS and provides a much better estimate than the no-model simulation for which $\mathcal{G}^{\text{No Model}} = 1.38\ \mathcal{G}^{\mathrm{DNS}}$.

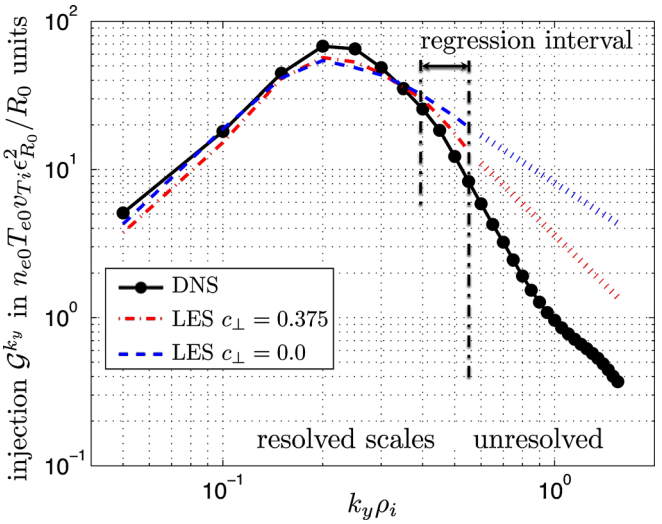

FIG. 6. (Color online) Free energy injection spectra $\mathcal{G}^{k_y}$ obtained with the model $c_\perp = 0.375$, compared with reference DNS and without model. Unresolved spectra of LES $c_\perp = 0.375$ and $c_\perp = 0.0$ have been constructed using a regression method with the assumption (24).

These power law parameters $\alpha_{x,y}$, computed using the above mentioned procedure, have to be taken with great care. They are useful to provide the estimates for global quantities such as the heat flux $\mathcal{G}$. Indeed, the global quantities have to be integrated over the entire wave vector spectrum. In LES, it is deliberately avoided to resolve all scales down to the end of the heat flux spectrum. As a consequence, it is opted here to use an extrapolation for the under-resolved scales. The unavoidable uncertainty on the power law parameters estimated here has, however, a rather limited impact on the value of global quantities, since these latter are strongly dominated by the resolved scales. For instance, from 80% up to 90% of the heat flux is carried on by the resolved scales.

On the contrary, the use of these power estimates to assess theoretical predictions would be much more hazardous. Indeed, in that case, the uncertainty on the power law exponents would very directly affect the comparison between LES results and theory and could strongly impact on the conclusions. Moreover, the range of resolved wave vectors available in the LES presented here is rather limited and does not really allow for such a comparison.

V. ROBUSTNESS OF THE LES APPROACH

The choice $c_\perp = 0.375$ has proven to give a reasonable agreement between the LES and the DNS predictions, in the case of standard CBC parameters. However, the LES methodology is only useful if the model parameters do not have to be calibrated for each set of parameters. In this section, it is proposed to explore the robustness of the LES approach by varying the logarithmic temperature gradient ω_{Ti}.

One of the most well known features of ITG turbulence is the Dimits shift,[22] i.e., a nonlinear upshift of the stability threshold with respect to a linear analysis. This upshift occurs when varying the values of the logarithmic temperature gradient ω_{Ti}, while keeping the logarithmic density gradient ω_{ni} constant. The explanation of such an effect is that turbulence nonlinearly transfers the free energy to the zonal flows (i.e., purely radial structures, corresponding to finite k_x, but $k_y = k_\parallel = 0$). These structures then suppress the ITG instability if its linear growth rate is not sufficiently large, and turbulence can not be driven even if the plasma is linearly unstable.

In Fig. 7, all the parameters characterizing the CBC have been kept constant, except the logarithmic temperature gradient which is varied from the standard CBC value of $\omega_{Ti} = 6.96$ to $\omega_{Ti} = 5.5$, 6.0, and 8.0. All simulations are performed using the model described in Eq. (17), with $c_\perp = 0.375$. The values $\omega_{Ti} = 6.0$ and $\omega_{Ti} = 5.5$ are close to the nonlinear threshold. It is then observed that an important part of the free energy is stored into the zonal flows. Such a result is in qualitative agreement with the usual picture of the Dimits shift.[25] On the contrary, when the temperature gradient is increased, the total free energy increases and peaks around $k_x\rho_i \sim 0.05$ and $k_y\rho_i \sim 0.15$.

Such a test shows that the LES approach can reproduce qualitatively the expected phenomenology at a much lower cost than the DNS. However, it is important to assess the quantitative agreement between LES and DNS. For this reason, an another comparison between LES and DNS has been performed for $\omega_{Ti} = 8.0$. As shown in Fig. 8, the LES using the same model with $c_\perp = 0.375$ again reproduces the resolved free energy spectra obtained from the DNS reasonably well. In particular, there is a clear improvement when compared with the no-model run. The value of $\omega_{Ti} = 8.0$ corresponds to a more turbulent state than $\omega_{Ti} = 6.96$, and the LES appears to be fairly well robust in this regime. It should be acknowledged, however, that the situation is not fully satisfactory when turbulence strength is decreased. For instance, in Fig. 9 ($\omega_{Ti} = 6.0$), the LES predictions, although still acceptable, start to deviate significantly from the DNS results in the large scale range. This is reminiscent of a difficulty known in the development of model for LES in fluid turbulence. Very few models are capable to capture correctly the transition between laminar and turbulent flows. Probably, the very simple model proposed here also suffers from such a deficiency.

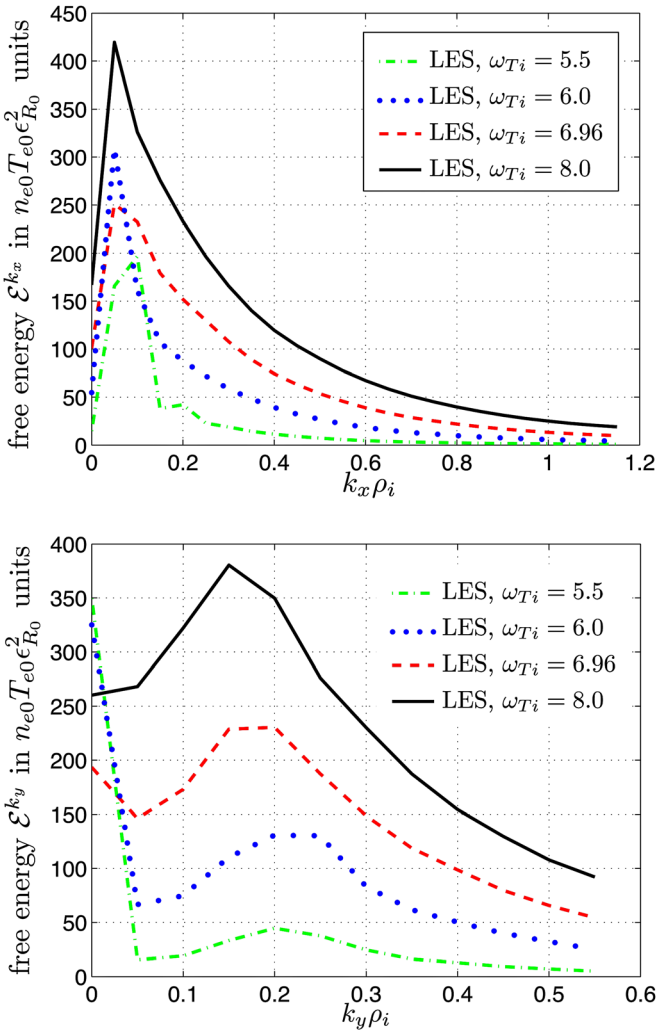

FIG. 7. (Color online) Resolved free energy spectra $\mathcal{E}^{k_x}$ (top) and $\mathcal{E}^{k_y}$ (bottom) obtained with the model (17) $c_\perp = 0.375$ for various values of the logarithmic temperature gradient ω_{Ti}.

VI. DISCUSSION

The study presented here shows that the concept of LES can be extended to three-dimensional (in space) gyrokinetics. The very good agreement reported in Figs. 3 and 8 between

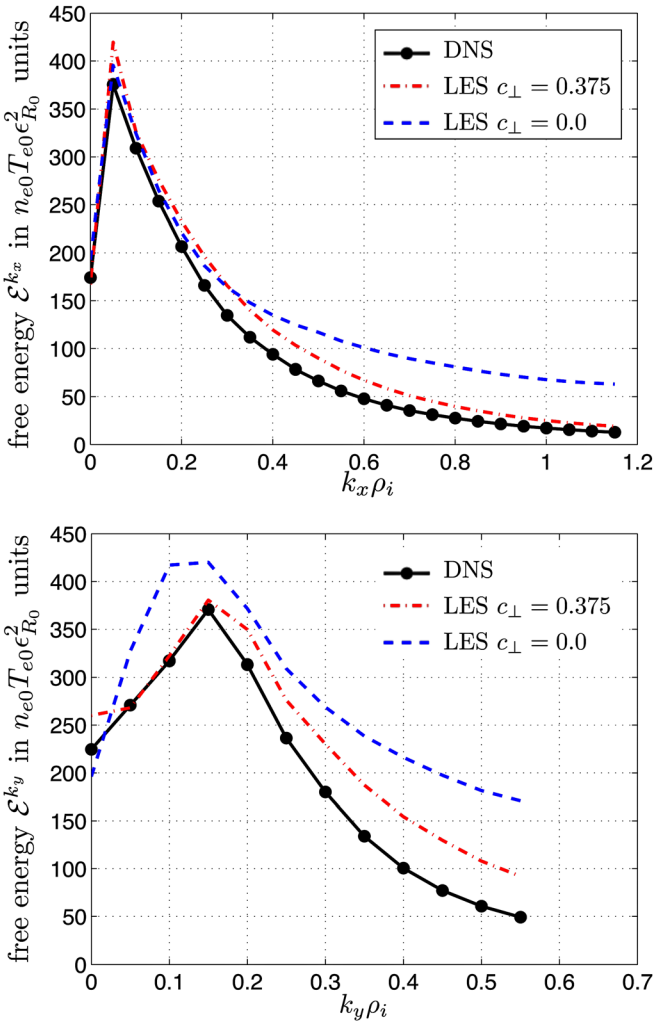

FIG. 8. (Color online) Resolved free energy spectra $\mathcal{E}^{k_x}$ (top) and $\mathcal{E}^{k_y}$ (bottom) obtained with the model (17) $c_\perp = 0.375$ for $\omega_{Ti} = 8.0$. Comparison with a highly resolved DNS with $\omega_{Ti} = 8.0$ and with LES without model.

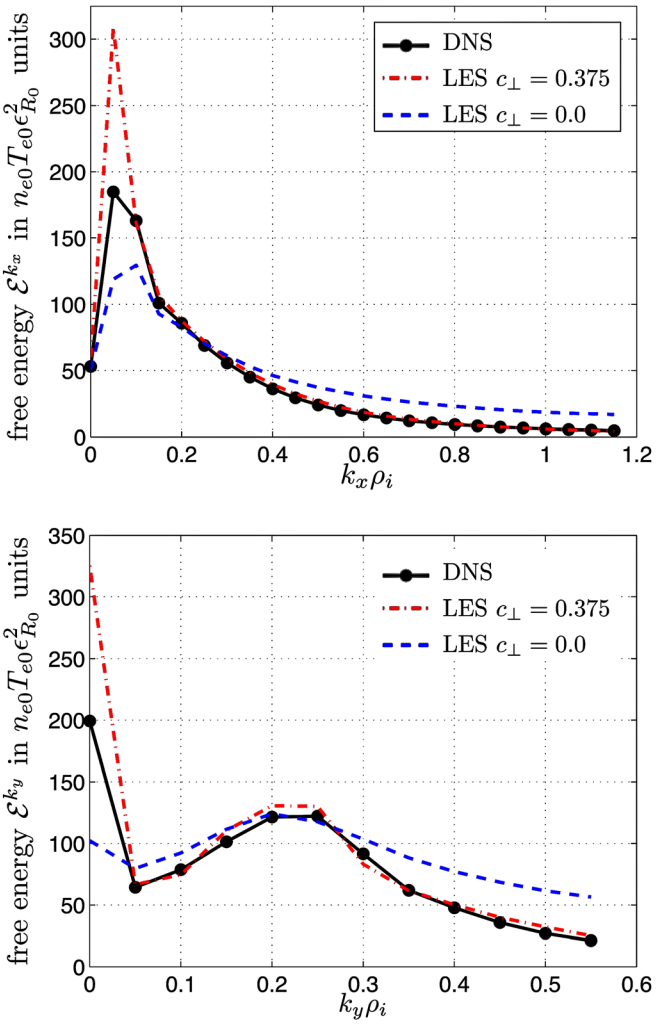

FIG. 9. (Color online) Same as Figure 8 with $\omega_{Ti} = 6.0$.

fully resolved simulations and under-resolved simulations including a simple model for the filtered scales is encouraging. It shows that the model, calibrated for a given value of the temperature gradient in ITG turbulence, is able to reproduce the large scale spectra of the free energy for higher temperature gradient. It should be noted that such a test is quite demanding since the free energy has to be reproduced for each scale. Hence, the model has not only be able to dissipate the correct amount of free energy, but it also has to distribute the dissipation correctly amongst the different scales.

It should be acknowledged, however, that the robustness of the model has not been proved in the most general sense. For instance, when the turbulence level is lowered by decreasing the parameter ω_{Ti}, the agreement between the under-resolved and the fully resolved simulations becomes less and less satisfactory—although such behavior can be understood and even anticipated since, for low ω_{Ti}, turbulence is not fully developed and the cascade picture starts to break down. An interesting extension of the present approach would then be to apply the dynamic procedure used to calibrate automatically the amplitude of sub-grid scale models in LES for fluid turbulence.[8] The dynamic procedure is known to be able to predict the transition between turbulence and laminar flows by automatically setting the model amplitude to zero in the laminar regime in which the small scales are not active. Hence, although the models are designed by using concepts valid for fully developed turbulence, the dynamic procedure seems to be able to extend their validity into totally different regimes. However, the implementation of the dynamic procedure in gyrokinetics is more intricate than the use of the simple model studied here.

The use of positive hyper-diffusion coefficients imposes a clear limitation to the model presented here. For instance, in certain cases an inverse cascade could be observed[26] and would definitively not be appropriately modelled by a positive hyper-diffusion term. The use of negative hyper-diffusion is, however, quite dangerous since it might lead to brutal instabilities in the code. The model could be extended to combine several terms proportional, for instance, to k_x^4 and k_y^4. In that case, one of the hyper-diffusion could be negative. This would perhaps be a good approach to model an inverse cascade driving anisotropy in the largest scales. Models attempting to represent an inverse transfer of energy (backscatter) in fluid turbulence using negative viscosity[27] or random forcing[28] have been suggested and could be used as a

guide in further development of LES for gyrokinetic equations.

Finally, it is interesting to discuss the computational gain obtained in the LES simulation presented in Sec. V. Although for the present case, the fully resolved reference simulation is not using a very large grid, the LES grid (and hence the required memory) can be reduced by 86%. In terms of central processing unit (CPU) time, the gain is even higher. Indeed, the simulation can be performed with a larger time step since the smallest scales are larger than in the reference simulation (in practice, with the grid resolution chosen in this study, the time step is increased by a factor of about two in the LES when compared to the DNS). As a consequence, the overall computational effort required for the LES runs appears to be more than 20 times smaller than in the DNS simulations. This finding indicates that the LES approach is quite promising in the context of gyrokinetics. Further studies along these lines, also exploring other types of plasma turbulence (driven, e.g., by trapped electron modes or electron temperature gradient modes), will be the focus of future work.

ACKNOWLEDGMENTS

The authors would like to thank G. W. Hammett, G. G. Plunk, T. Tatsuno, and D. R. Hatch for very fruitful discussions. We gratefully acknowledge that the results in this paper have been achieved with the assistance of high performance computing resources on the HPC-FF system at Jülich, Germany. This work has been supported by the contract of association EURATOM—Belgian state.

[1]A. A. Schekochihin, S. C. Cowley, W. Dorland, G. W. Hammett, G. G. Howes, G. G. Plunk, E. Quataert, and T. Tatsuno, Plasma Phys. Controlled Fusion **50**, 124024 (2008).
[2]T. Tatsuno, M. Barnes, S. C. Cowley, W. Dorland, G. G. Howes, R. Numata, G. G. Plunk, and A. A. Schekochihin, Phys. Rev. Lett. **103**, 015003 (2009).
[3]G. G. Plunk, Ph. D. thesis, University of California Los Angeles, 2009.
[4]G. G. Plunk, S. C. Cowley, A. A. Schekochihin, and T. Tatsuno, J. Fluid Mech. **664**, 407 (2010).
[5]A. Bañón Navarro, P. Morel, M. Albrecht-Marc, D. Carati, F. Merz, T. Görler, and F. Jenko, Phys. Rev. Lett. **106**, 055001 (2011).
[6]D. R. Hatch, P. W. Terry, F. Jenko, F. Merz, and W. M. Nevins, Phys. Rev. Lett. **106**, 115003 (2011).
[7]J. Smagorinsky, Mon. Weather Rev. **91**, 99 (1963).
[8]M. Germano, U. Piomelli, P. Moin, and W. H. Cabot, Phys. Fluids A **3**, 1760 (1991).
[9]A. J. Brizard and T. S. Hahm, Rev. Mod. Phys. **79**, 421 (2007).
[10]X. Garbet, Y. Idomura, L. Villard, and T. H. Watanabe, Nucl. Fusion **50**, 043002 (2010).
[11]O. Agullo, W.-C. Müller, B. Knaepen, and D. Carati, Phys. Plasmas **8**, 3502 (2001).
[12]B. Knaepen and P. Moin, Phys. Fluids **16**, 1255 (2004).
[13]S. A. Smith and G. W. Hammett, Phys. Plasmas **4**, 978 (1997).
[14]F. Jenko, W. Dorland, M. Kotschenreuther, and B. N. Rogers, Phys. Plasmas **7**(5), 1904 (2000).
[15]T. Dannert and F. Jenko, Phys. Plasmas **12**, 072309 (2005).
[16]F. Merz, Ph.D. thesis, Universität Münster, 2009.
[17]M. A. Beer, S. C. Cowley, and G. W. Hammett, Phys. Plasmas **2**(7), 2687 (1995).
[18]X. Lapillone, S. Brunner, T. Dannert, S. Jolliet, A. Marinoni, L. Villard, T. Görler, F. Jenko, and F. Merz, Phys. Plasmas **16**, 032308 (2009).
[19]T.-H. Watanabe and H. Sugama, Nucl. Fusion **46**, 24 (2006).
[20]J. Candy and R. E. Waltz, Phys. Plasmas **13**, 032310 (2006).
[21]T.-H. Watanabe and H. Sugama, Phys. Plasmas **11**, 1476 (2004).
[22]A. M. Dimits, G. Bateman, M. A. Beer, B. I. Cohen, W. Dorland, G. W. Hammett, C. Kim, J. E. Kinsey, M. Kotschenreuther, A. H. Kritz, L. L. Lao, J. Mandrekas, W. M. Nevins, S. E. Parker, A. J. Redd, D. E. Shumaker, R. Sydora, and J. Weiland, Phys. Plasmas **7**, 969 (2000).
[23]M. J. Pueschel, T. Dannert, and F. Jenko, Comput. Phys. Commun., **181** 1428 (2010).
[24]T. Görler and F. Jenko, Phys. Plasmas **15**, 102508 (2008).
[25]K. Itoh, S.-I. Itoh, P. H. Diamond, T. S. Hahm, A. Fujisawa, G. R. Tynan, M. Yagi, and Y. Nagashima, Phys. Plasmas **13**, 055502 (2006).
[26]Y. Idomura, Phys. Plasmas **13**, 080701 (2006).
[27]A. Chekhlov, S. A. Orszag, S. Sukoriansky, B. Galerpin, and I. Staroselsky, Physica D **98**, 321 (1996).
[28]D. Carati, S. Ghosal, and P. Moin, Phys. Fluids **7**, 606 (1995).